Visible Derivative Spectroscopy of Multispectral and Hyperspectral Images: A New Approach to Algal and Cyanobacterial Differentiation

Dr. Joseph Ortiz

(jortiz@kent.edu),

Kent State University

Department of Geology

Collaborators: D. Avouris (KSU), Stephen Schiller (SDSU), **Jeff Luvall (NASA-Marshall)**, John Lekki, RogerTokars, Robert Anderson, Robert Shuchman, Michael Sayers, and Richard Becker

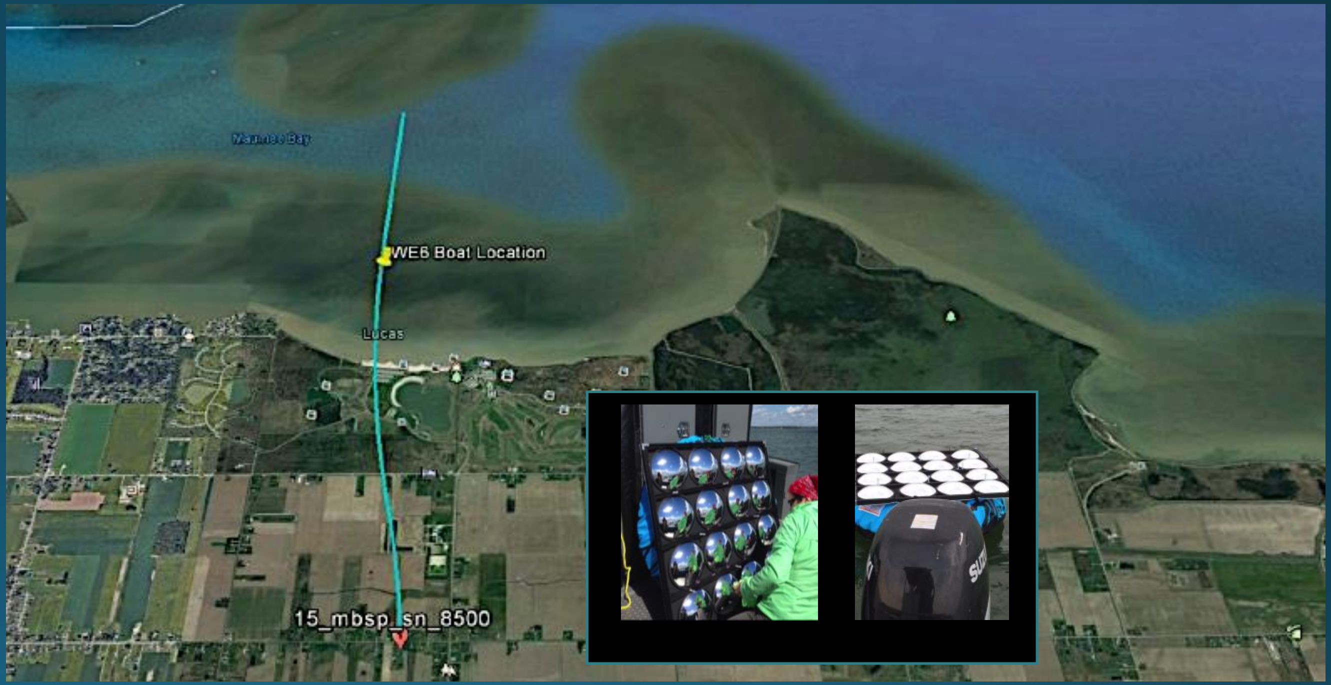

Peer-Reviewed article: https://www.frontiersin.org/articles/10.3389/fmars.2017.00296/full

Thanks to…

Funding :

- ✧ Old Woman Creek NERR, Ohio Sea Grant, NASA Glenn, Ohio Board Higher Education

Research Access:

- ✧ USGS, Ohio EPA, NOAA, ODNR Watercraft Division, Cleveland Water

Collaborators:

- ✧ NASA Glenn (Lekki, Tokars, Ansari, Liou), OhioView Institutions (Becker, Simic, Wei, Liu)
- ✧ USGS LEBS (Richard Kraus)
- ✧ NASA MSFC (Jeff Luvall), SDSU (Stephen Schiller)
- ✧ NOAA GLERL/MTRI (Leshkevich, Shuchman)
- ✧ Donna Witter, Sapphire Geoscience Informatics
- ✧ Khalid Adem Ali, College of Charleston
- ✧ Sushma Parab, KSU Postdoc
- ✧ Nick Tufillaro and Curtis Davis, Theo Dreher
  - ✧ Hyperspectral Imager for Coastal Oceanography (HICO) Oregon State University
- ✧ Mandy Razzano, Ohio EPA
- ✧ Students: N. Bonini, Dulci Avouris, R. Craine, J. Sadallah, N. Wijikoon, D. Fuecht, K. Hollister and others

Water Quality Monitoring by Remote Sensing? The problem…

- Remote sensing of lake color gives information on plant biomass, but…
- Lake water is a complex "organic soup"
  - Various types of algae and cyanobacteria
  - Colored dissolved organic matter
  - Suspended sediment
- Collect Hyperspectral swaths in Western basin of Lake Erie using NASA Glenn HSI2
- Apply KSU Spectral decomposition method
  - Varimax-rotated, Principal Component Analysis
  - Eigenvector-eigenvalue decomposition
  - Soft unsupervised classification method

All natural samples are mixtures!

Ortiz et al., (HyspIRI 2017; jortiz@kent.edu)

We apply 4 different variations on the Empirical Line Method (ELM) method to reflectance :

ELM0 method uses two instruments (HSI2 and ASD HH2) along with mirrors. Ratio HSI2 water pixels to mirror pixels to remove the atm. Then rescale using ASD HH2 data.

ELM2 method uses two instruments (HSI2 and ASD HH2) surface measurements of reflectance, diffuse to global ratio, and radiative transfer theory to get slope and intercept for water surface and mirror surface pair to go from radiance to reflectance.

The ELM1 method is ELM2 with the intercept term removed to test sensitivity of the VPCA to path radiance impact

The MTRI (Michigan Technological Research Institute) correction method uses three instruments (HSI2, upward looking ASD HH2, and downward looking HH2) The HSI2 and upward looking ASDHH2 provide at-sensor reflectance and then the downward looking HH2 uses a blacktop reference spectra to reshape the at-sensor reflectance to at-surface reflectance

Because the Varimax-rotated, Principal Component Analysis (VPCA) method is based on spectral shapes, it should be relatively insensitive to the quality of the atmospheric correction

ELM method Reflectance and VPCA

- Apply 4 variations of the Empirical Line Method for Atm correction
- How sensitive is the VPCA method to differences in atmospheric correction?

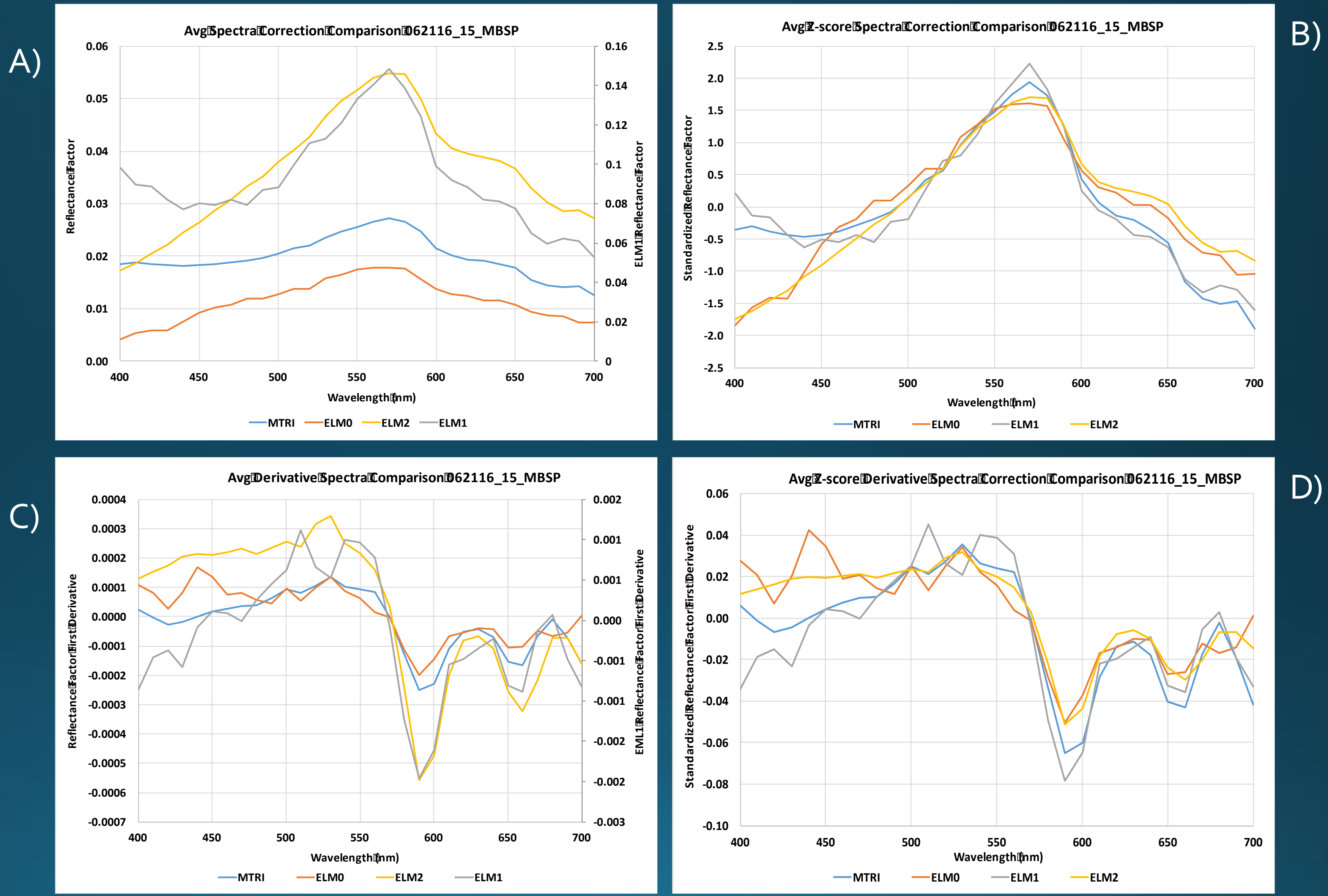

Figure 7

Ortiz et al., (HyspIRI 2017; jortiz@kent.edu)

Figure 8

062116 15_MBSP (10nm, SPEAR0, smooth9, various reflectance transform, georef) VPCA Pattern A

A) Uncorrected RGB (radiance) B) NOAA CI C) MTRI 6VPCA 1: 56% D) ELM0 5VPCA 1: 67.1% E) ELM1 4VPCA -1: 36.9% F) ELM2 4VPCA -1: 36.9%

G) Pattern A Loadings

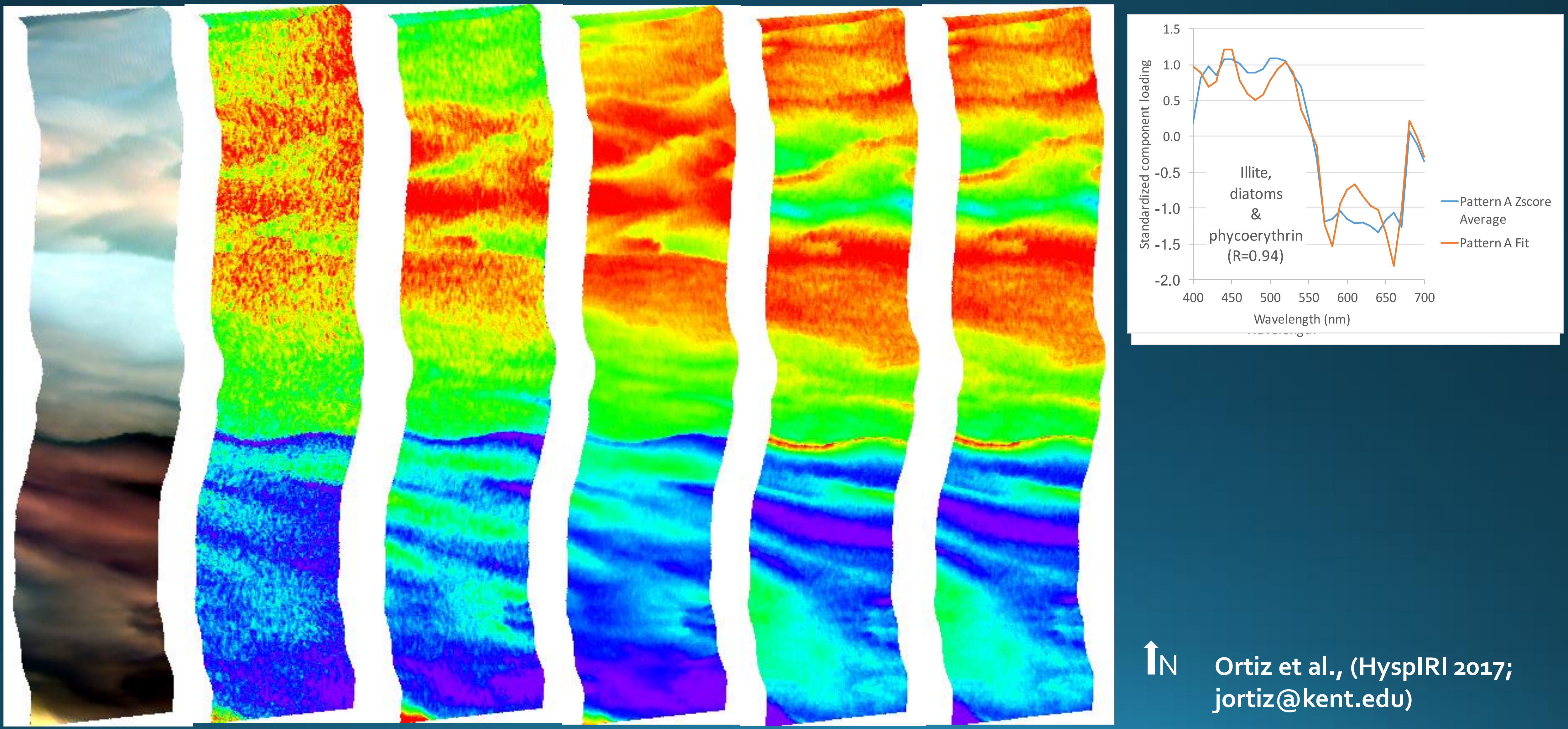

Ortiz et al., (HyspIRI 2017; jortiz@kent.edu)

Figure 9

062116 HSI2 Swath 15_MBSP: Pattern B

A) MTRI 6VPCA 2: 16.4% B) ELM0 5VPCA 2: 15.5% C) ELM1 4VPCA 3: 26.3% D) ELM2 4VPCA 3: 26.3%

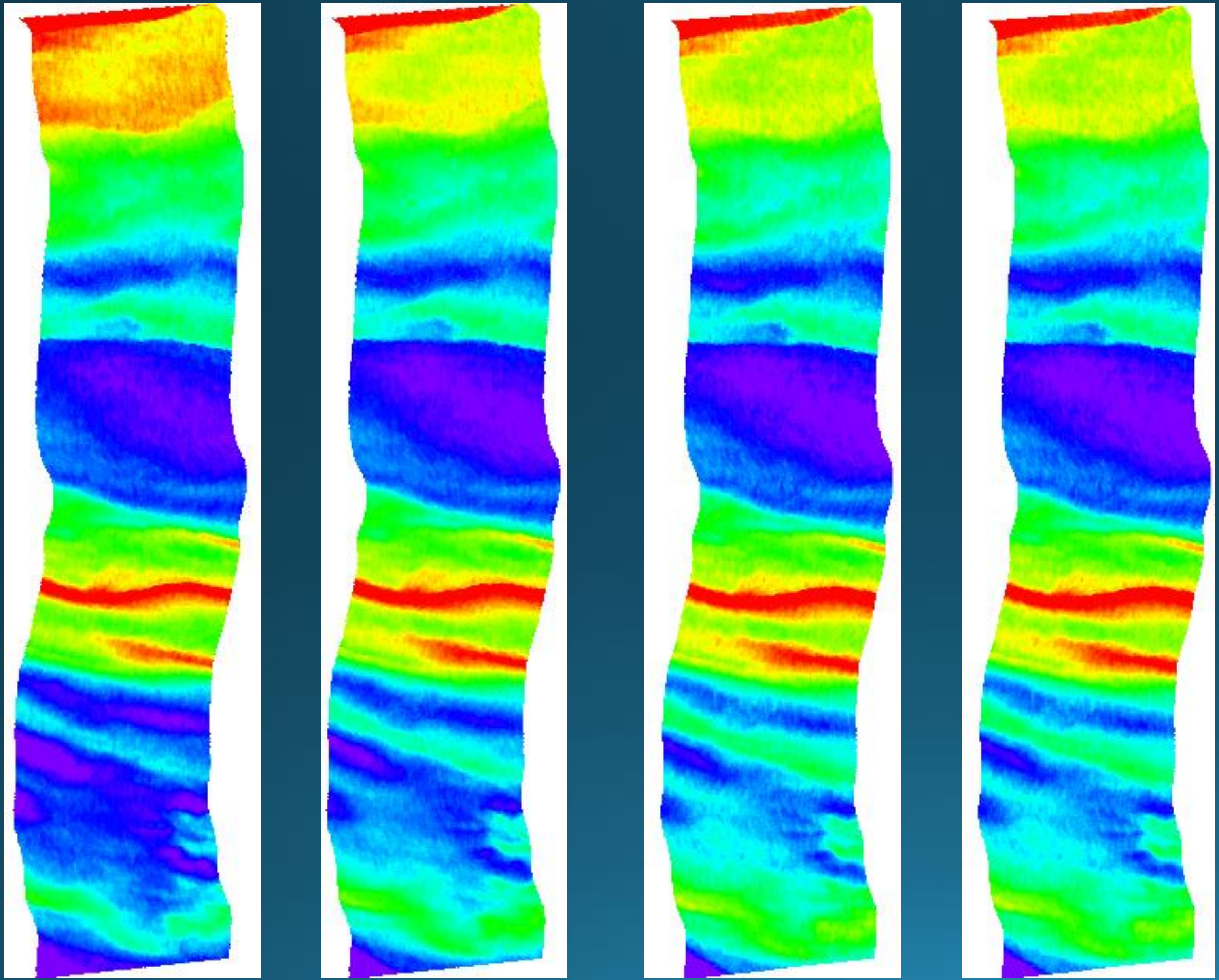

E) Pattern B Loadings

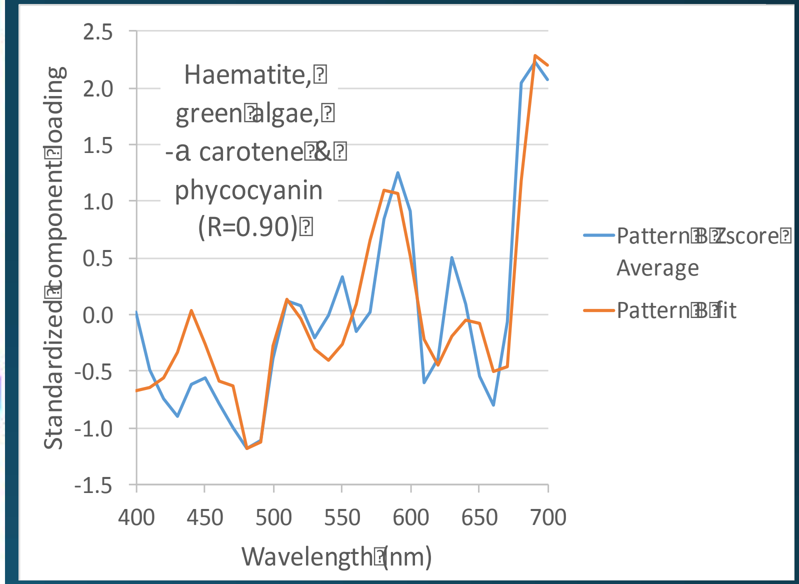

N

Ortiz et al., (HyspIRI 2017; jortiz@kent.edu)

Figure 10

062116 HSI2 Swath 15_MBSP: Pattern C

A) MTRI 6VPCA -3: 10% B) ELM0 5VPCA 3: 7.2% C) ELM1 4VPCA 2: 26.5% D) ELM2 4VPCA 2: 26.5%

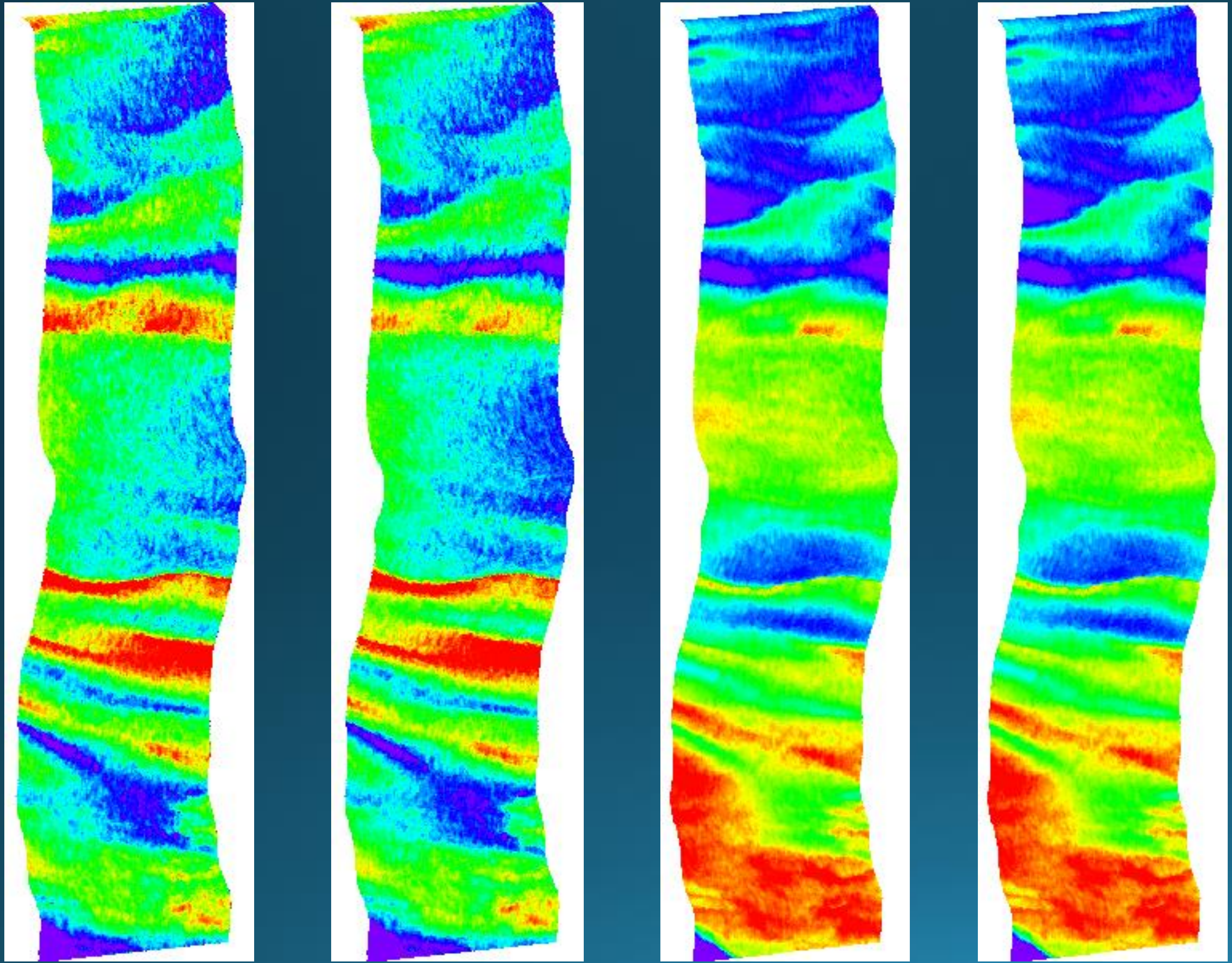

E) Pattern C Loadings

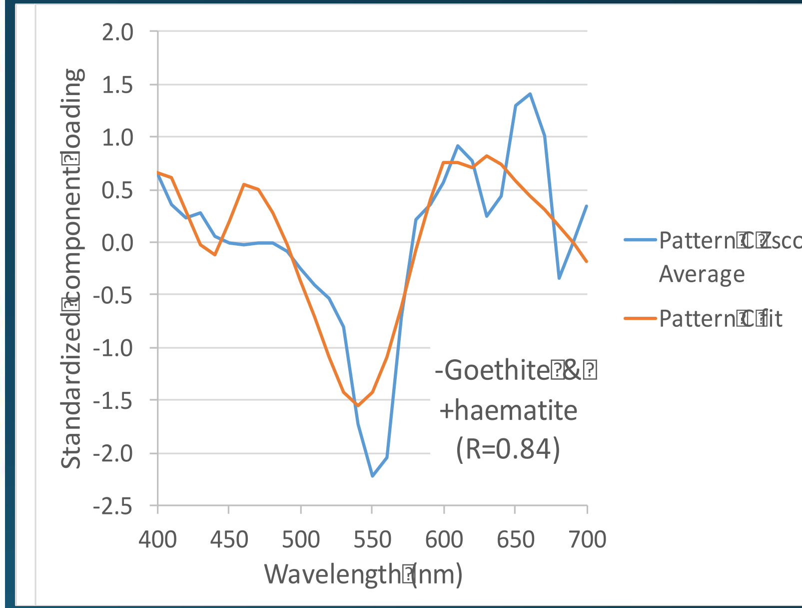

↑N

Ortiz et al., (HyspIRI 2017; jortiz@kent.edu)

Figure 11

062116 HSI2 Swath 15_MBSP: Pattern D

A) MTRI 6VPCA -4: 7.8% B) ELM0 5VPCA 4: 6.4% C) ELM1 4VPCA D) ELM2 4VPCA

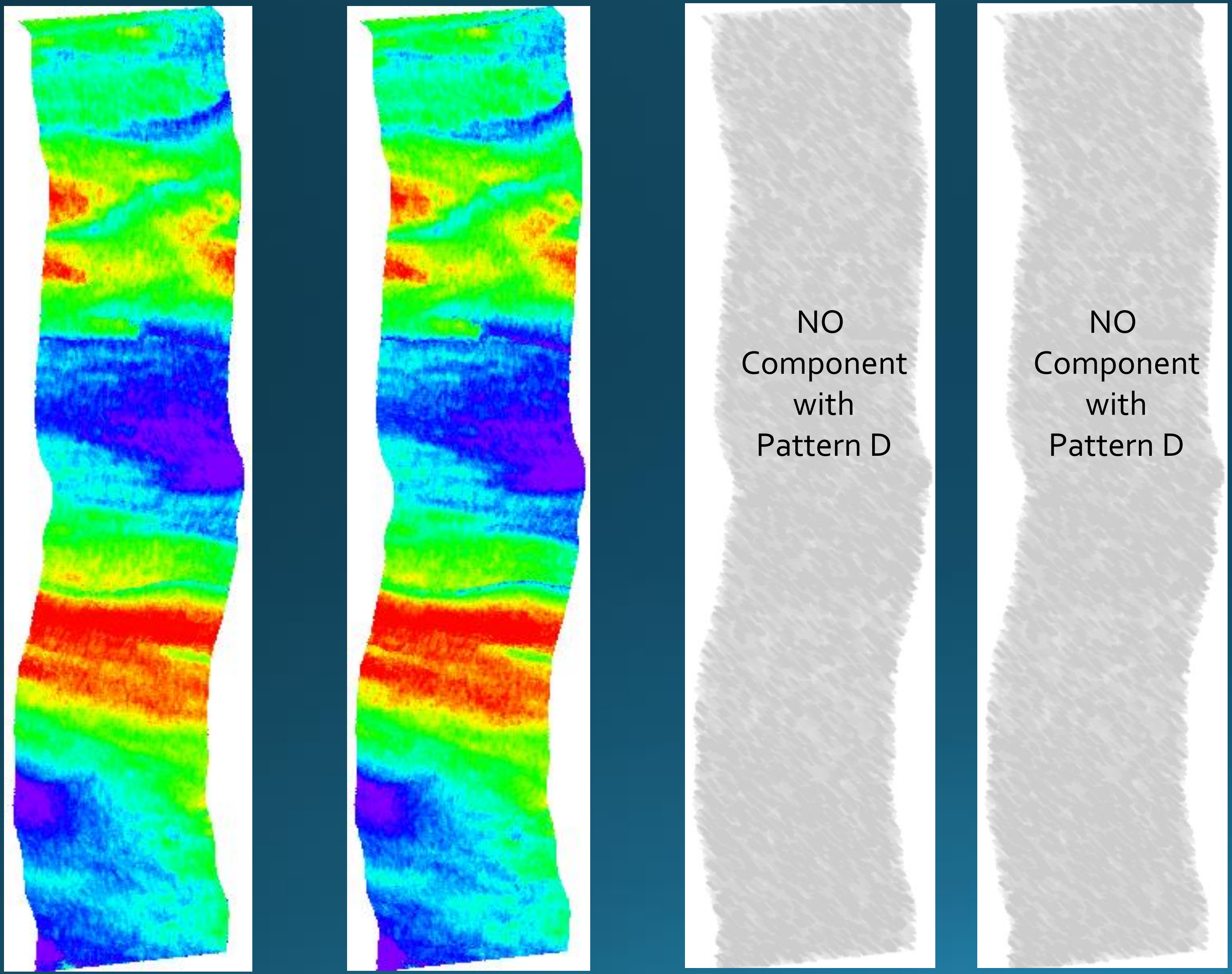

E) Pattern D Loadings

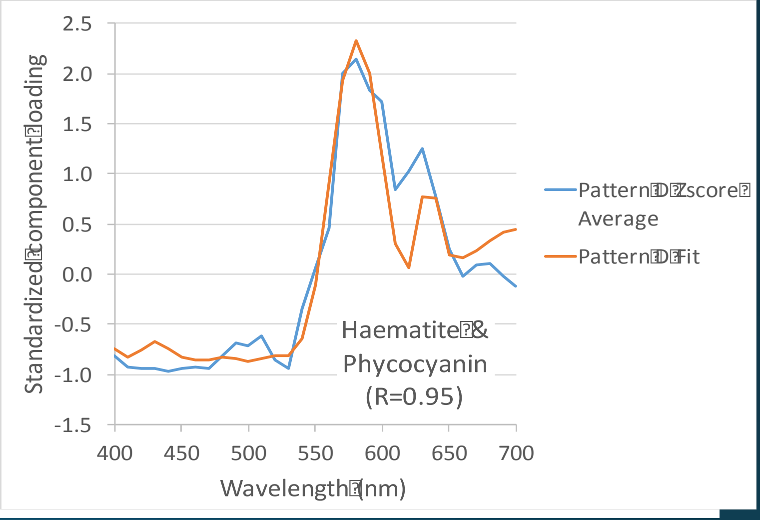

N

Ortiz et al., (HyspIRI 2017; jortiz@kent.edu)

Figure 13

062116 HSI2 Swath 15_MBSP: Pattern F

A) MTRI 6VPCA 6: 1.3%

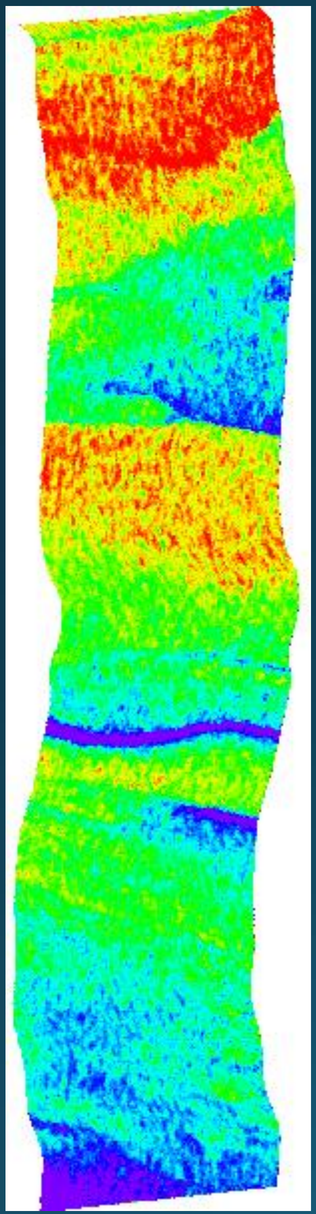

B) ELM0 5VPCA 5: 1%

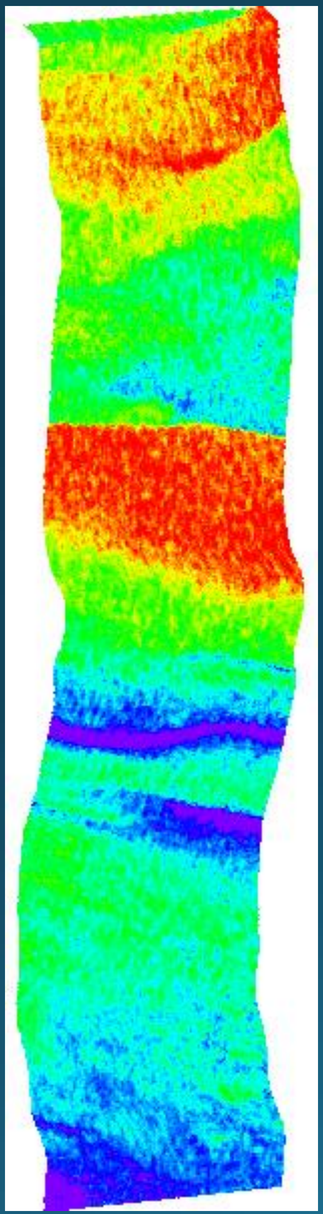

C) ELM1 4VPCA

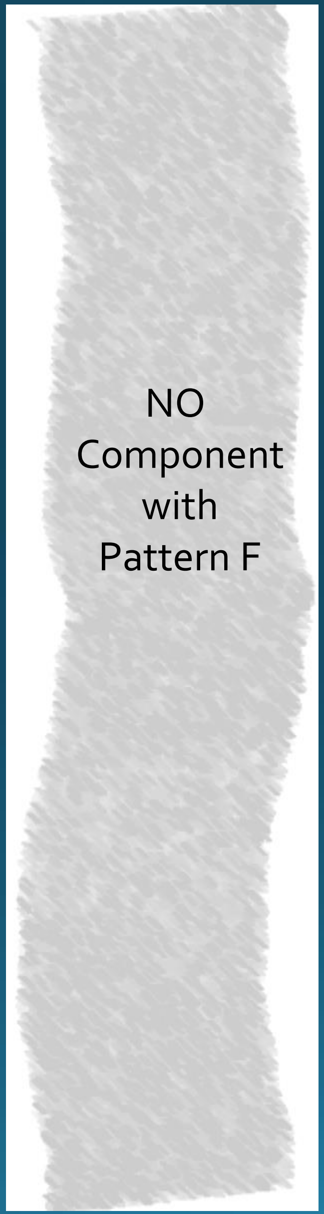

D) ELM2 4VPCA

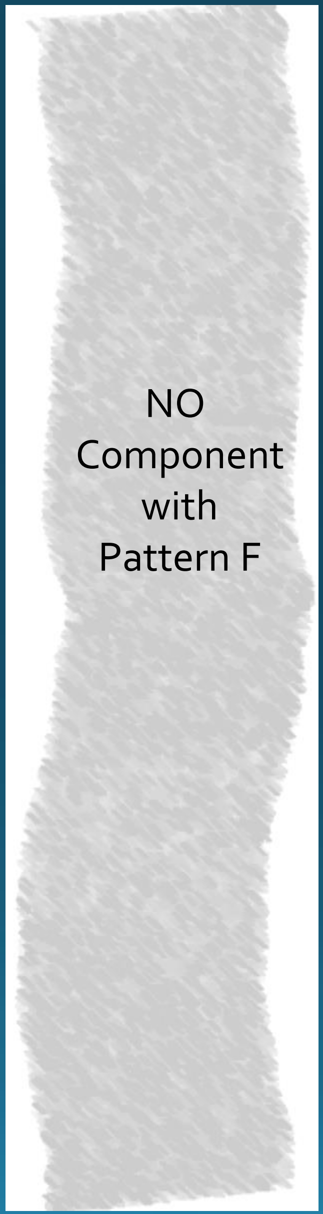

E) Pattern F Loadings

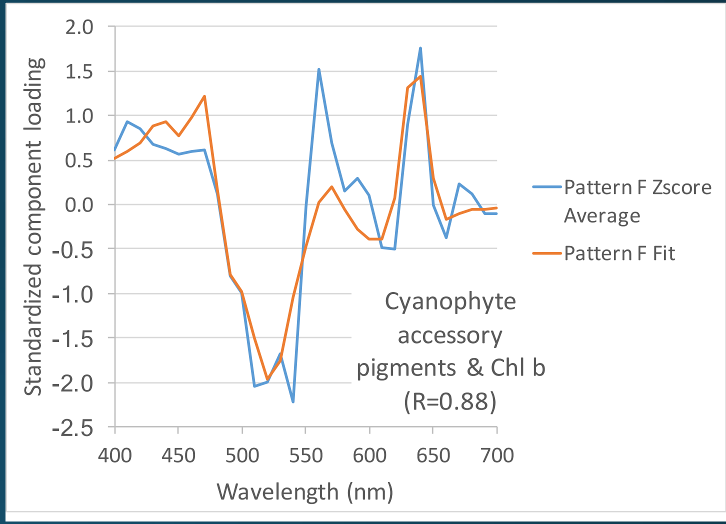

↑N

Ortiz et al., (HyspIRI 2017; jortiz@kent.edu)

Figure 12

062116 HSI2 Swath 15_MBSP: Pattern E

A) MTRI 6VPCA 5: 4.4% B) ELM0 5VPCA C) ELM1 4VPCA -4: 4.2% D) ELM2 4VPCA -4: 4.2%

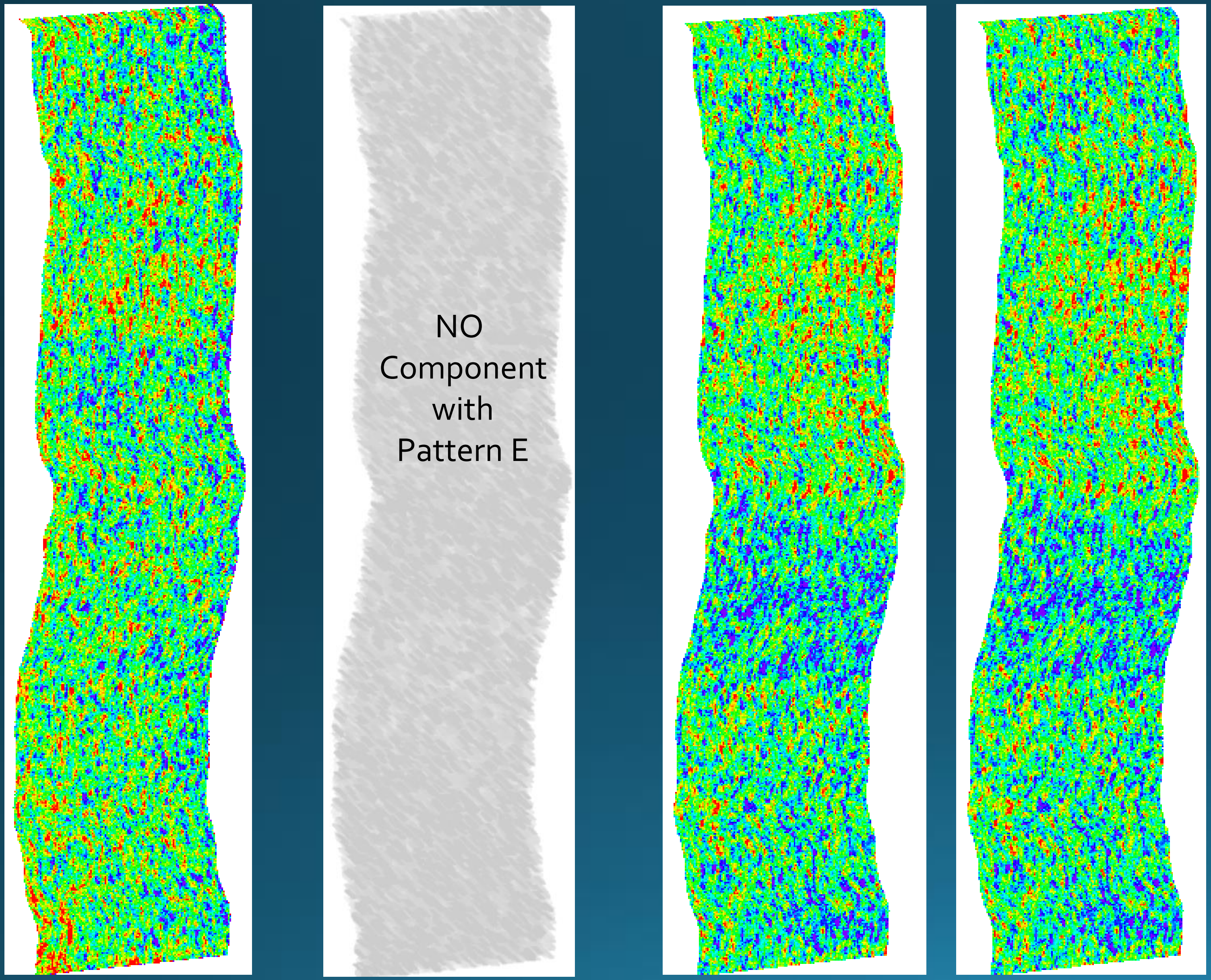

E) Pattern E Loadings

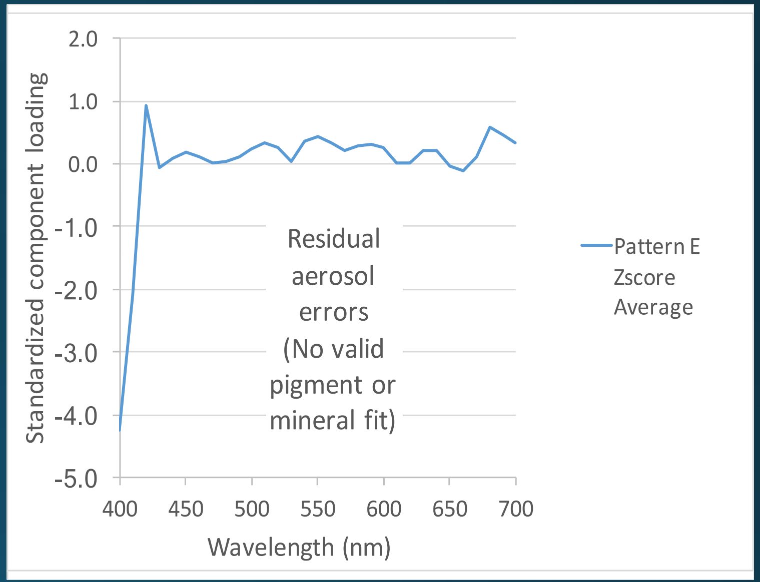

N

Ortiz et al., (HyspIRI 2017; jortiz@kent.edu)

062116 HSI2 15_MBSP: SPEAR0; MTRIcorr; L8 band res; L8 ground res

Dealing with Mixed Pixels

Q: How does the amount of information we can extract from Landsat 8 compare with Hyperspectral data sets?

A: Test w/ KSU Spectral decomposition method

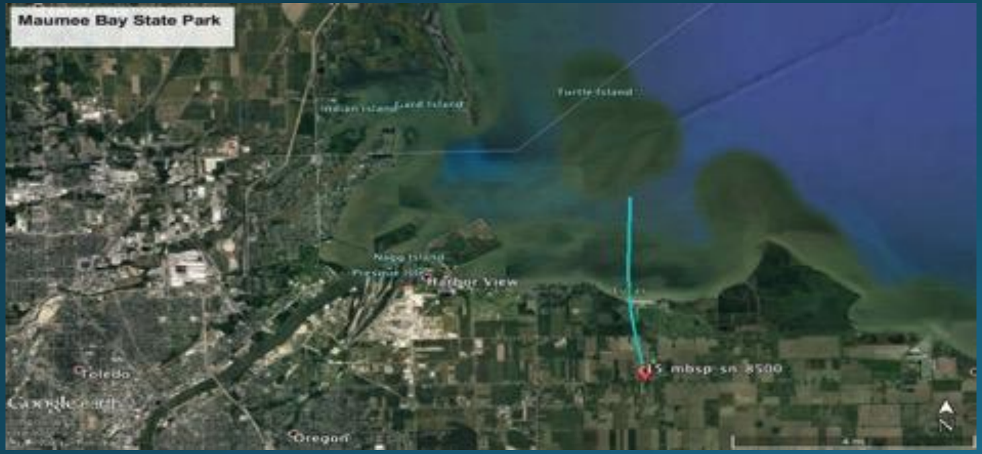

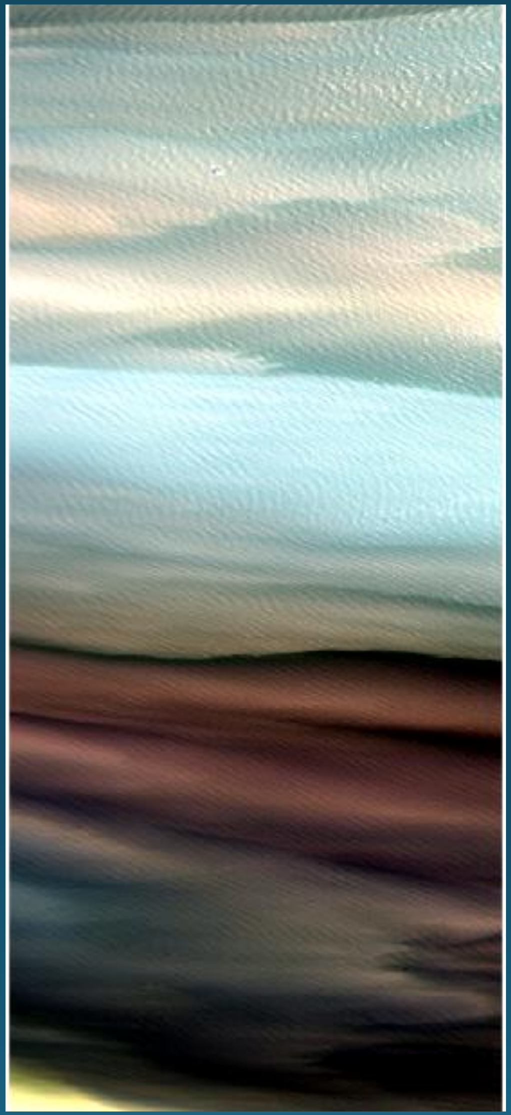

HSI2 Swath 15_MBSP at Landsat 8 band resolution, HSI2 ground resolution (3m). RGB

N

HSI2 Swath 15_MBSP at Landsat 8 band and ground (30m) resolution. RGB of resampled data

Ortiz et al., (HyspIRI 2017; jortiz@kent.edu)

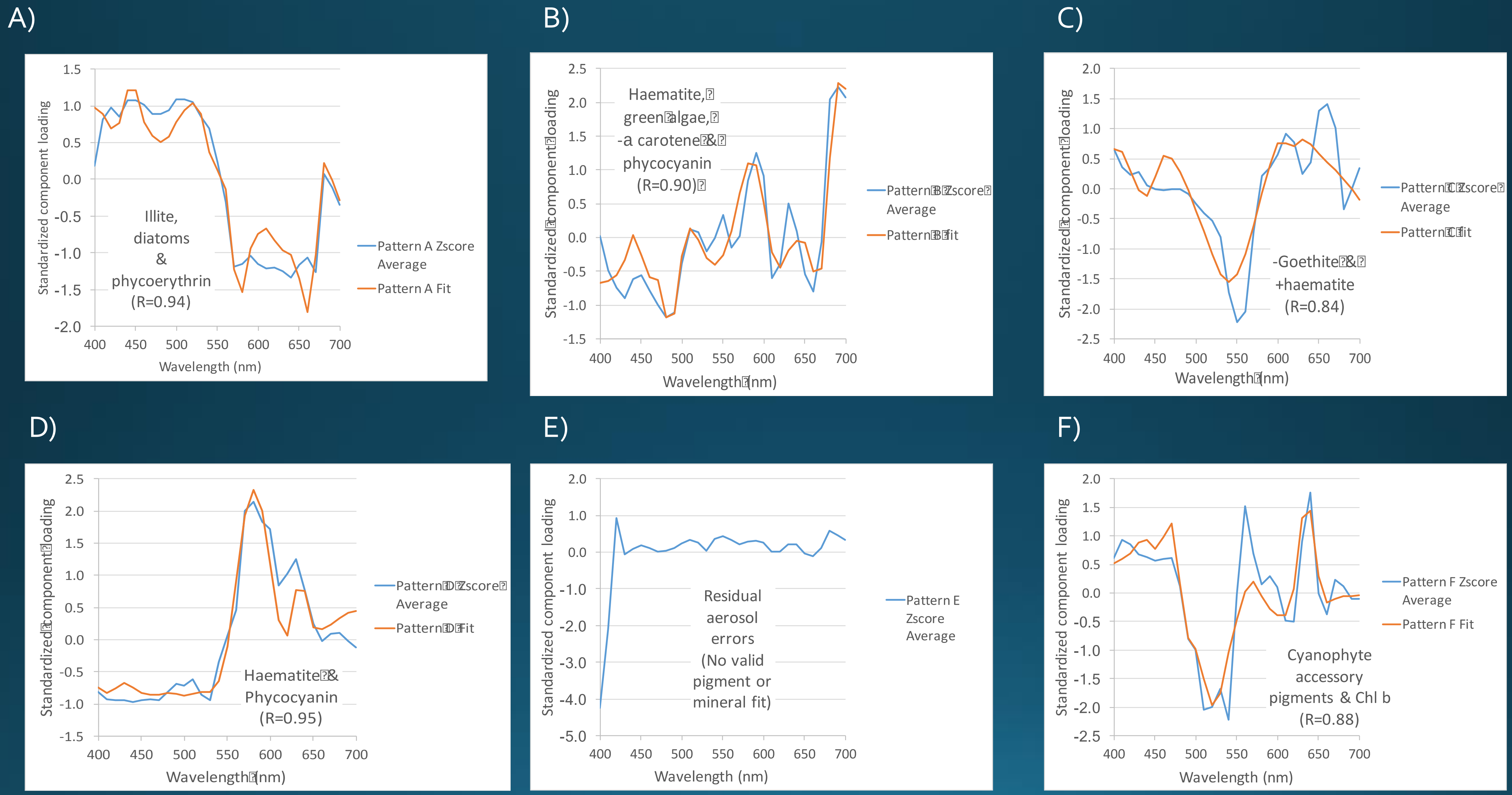

Figure 14 Z-score Loadings

Ortiz et al., (HyspIRI 2017; jortiz@kent.edu)

KSU Spectral Unmixing Experimental Design

Spectral Placement and Resolution	Spatial Resolution	
Landsat 8: Four bands: 440, 480, 560, 655 @ 20, 60, 60 and 30 nm resolution	30 m (simulated)	3 m (simulated)
NASA HSI2: 31 Bands 400-700 nm @10nm resolution	30 m (simulated)	3 m

Ortiz et al., (HyspIRI 2017; jortiz@kent.edu)

062116 HSI2 swath 15: SPEAR0; MTRIcorr; 10nm; 3m – smooth9 pixels: **5VPCA**

A) RGB

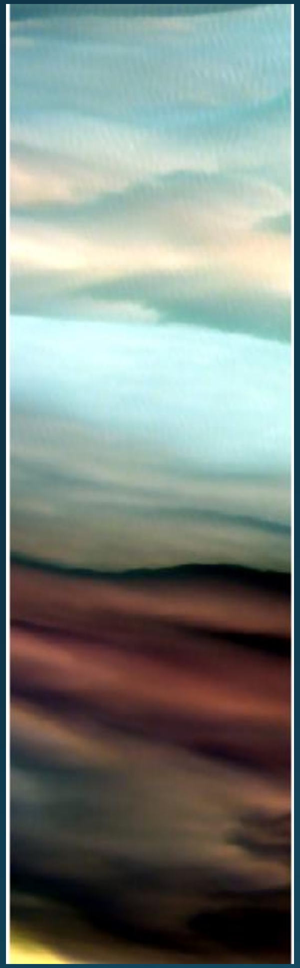

B) MTRI 6VPCA 1: 55.8%

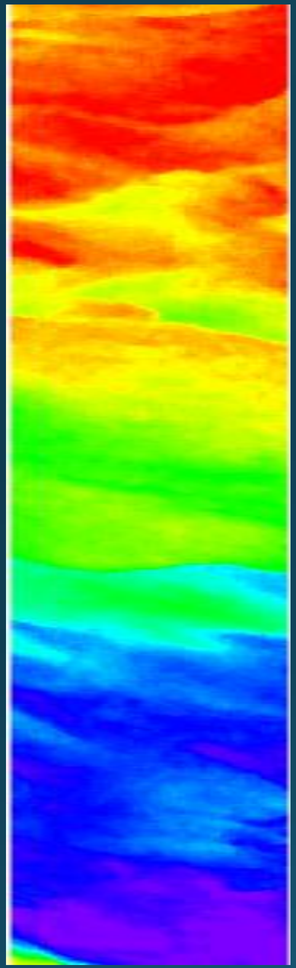

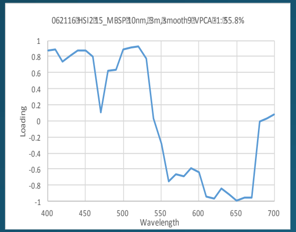

C) MTRI 6VPCA 2: 24.9%

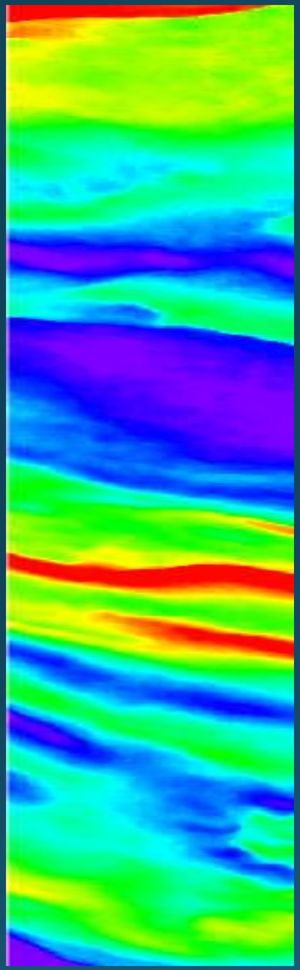

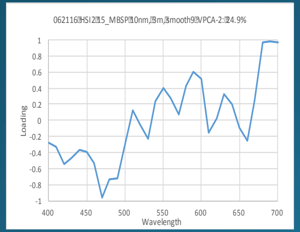

D) MTRI 6VPCA -3: 11.9%

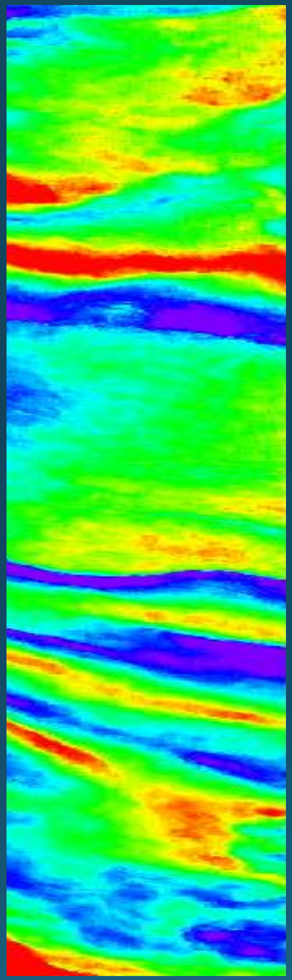

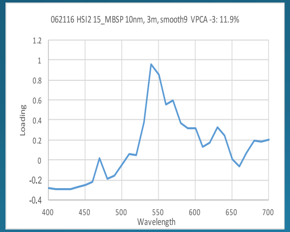

E) MTRI 6VPCA 4: 3.6%

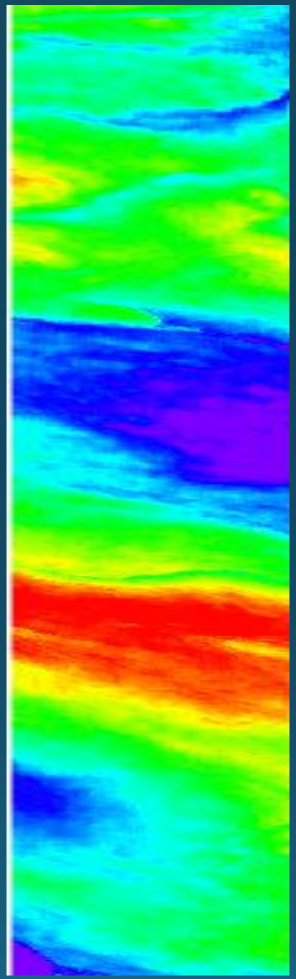

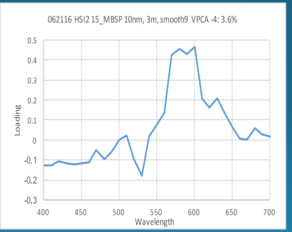

F) MTRI 6VPCA 5: 1.8%

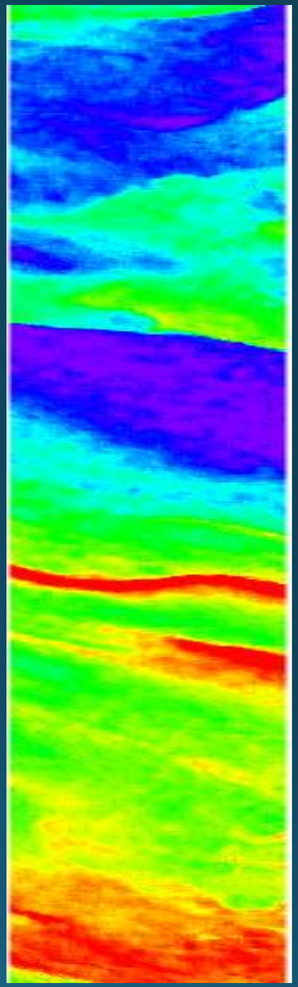

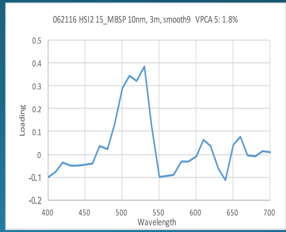

N

KSU Spectral Unmixing Experimental Outcome

Spectral Placement and Resolution	Number of Components extracted	
	30m	3m
Landsat 8: Four bands: 440, 480, 560, 655 @ 20, 60, 60 and 30 nm resolution	3	3
NASA HSI2: 31 Bands 400-700 nm @10nm resolution	5	5

Ortiz et al., (HyspIRI 2017; jortiz@kent.edu)

VPCA 1 Simulated L8 bands, 30m

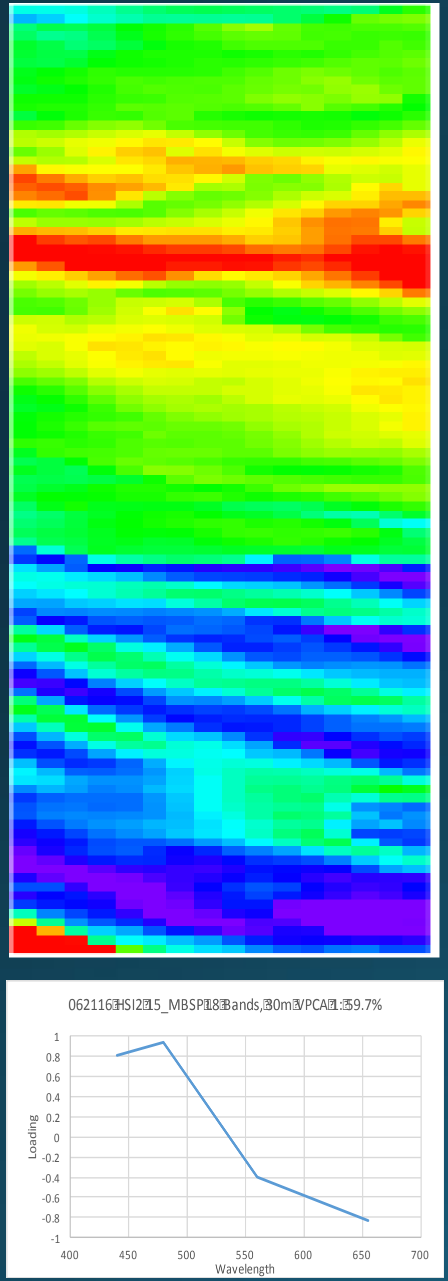

VPCA 1 Simulated L8 bands, 3m, Smooth 9x9

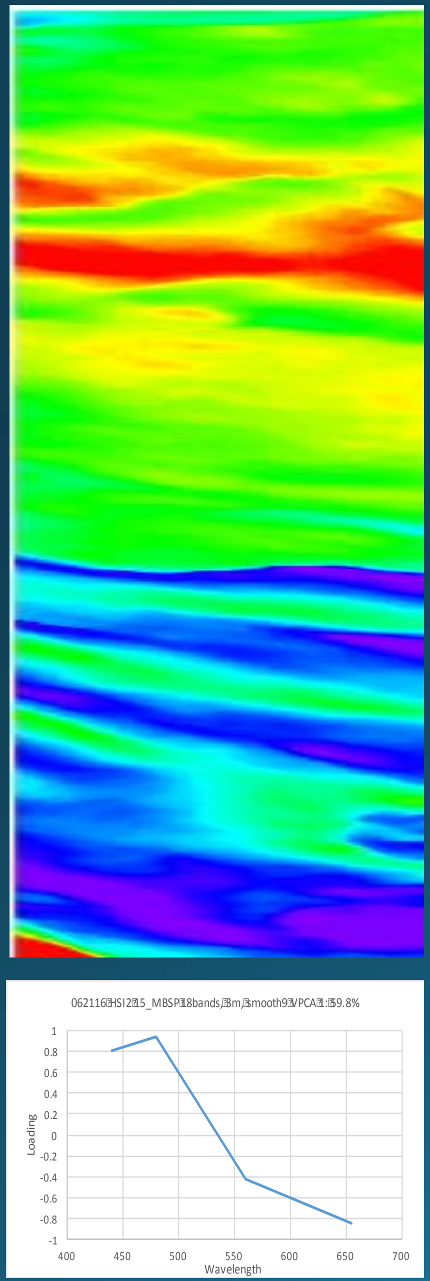

VPCA -1 HSI2 10nm, 30 m

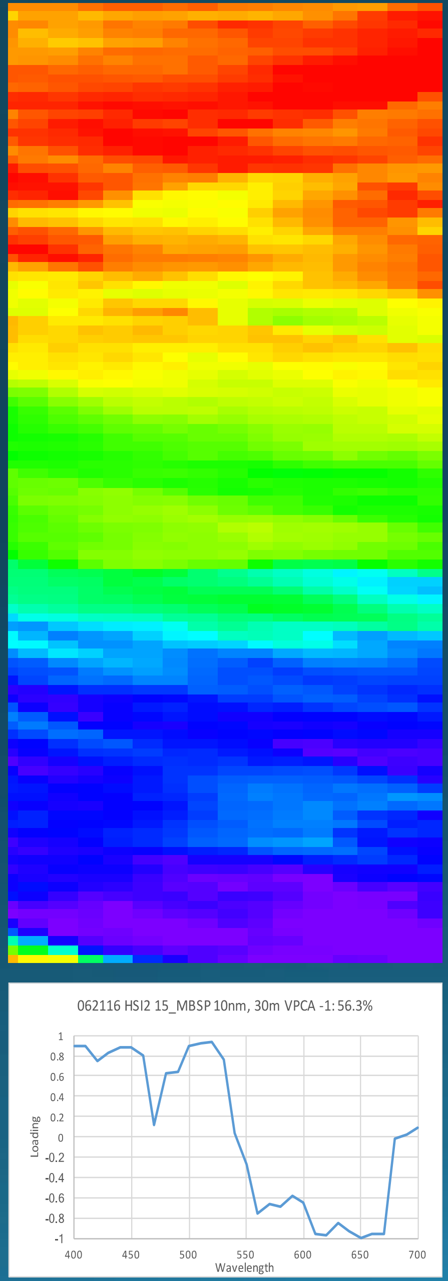

VPCA1 HSI2 10nm, 3 m, Smooth 9x9

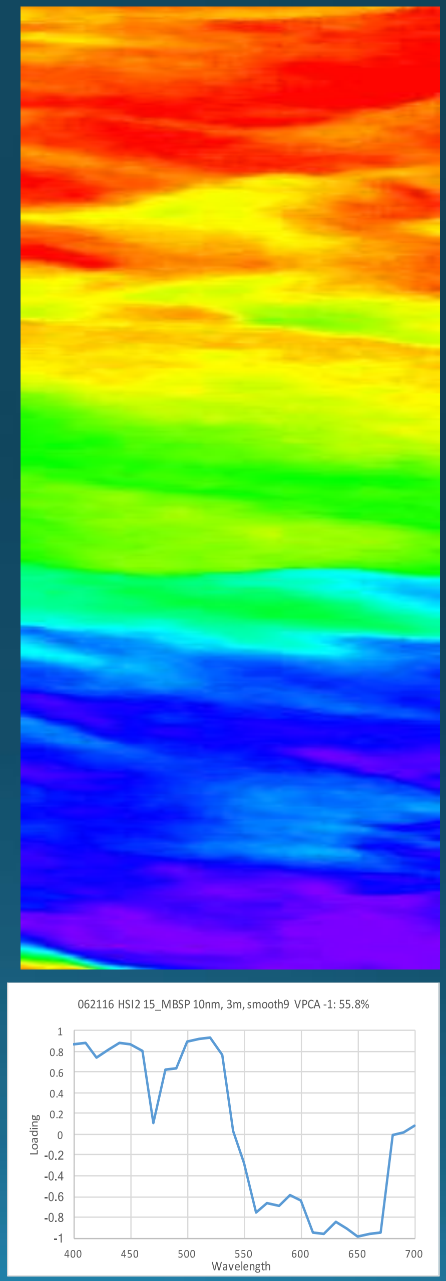

Composition:
Illite,
diatoms and
phycoerythrin
(R=0.94)

N

Ortiz et al., (HyspIRI 2017; jortiz@kent.edu)

VPCA 2 Simulated L8 bands, 30m

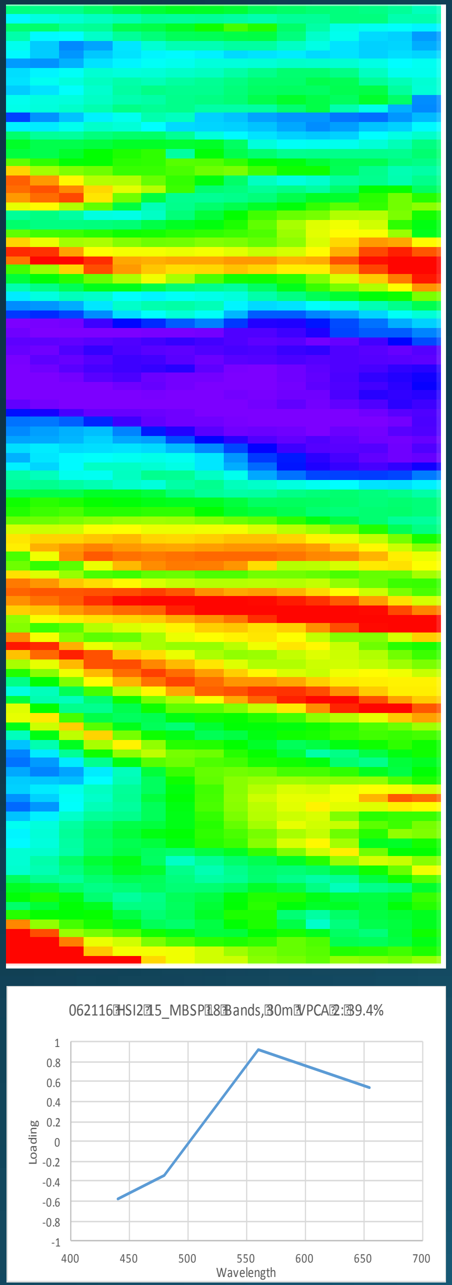

VPCA 2 Simulated L8 bands, 3m, Smooth 9x9

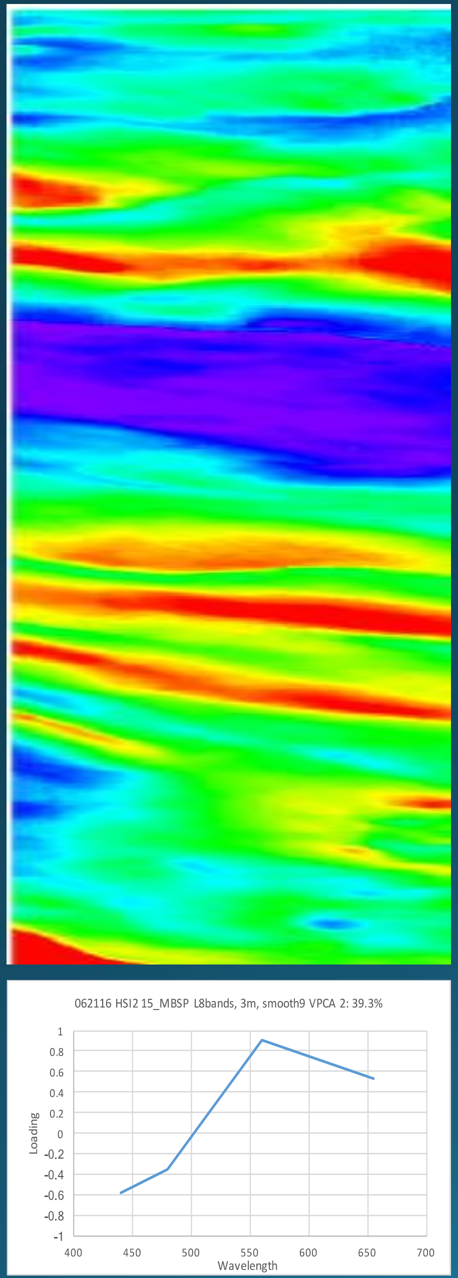

VPCA 2 HSI2 10nm, 30 m

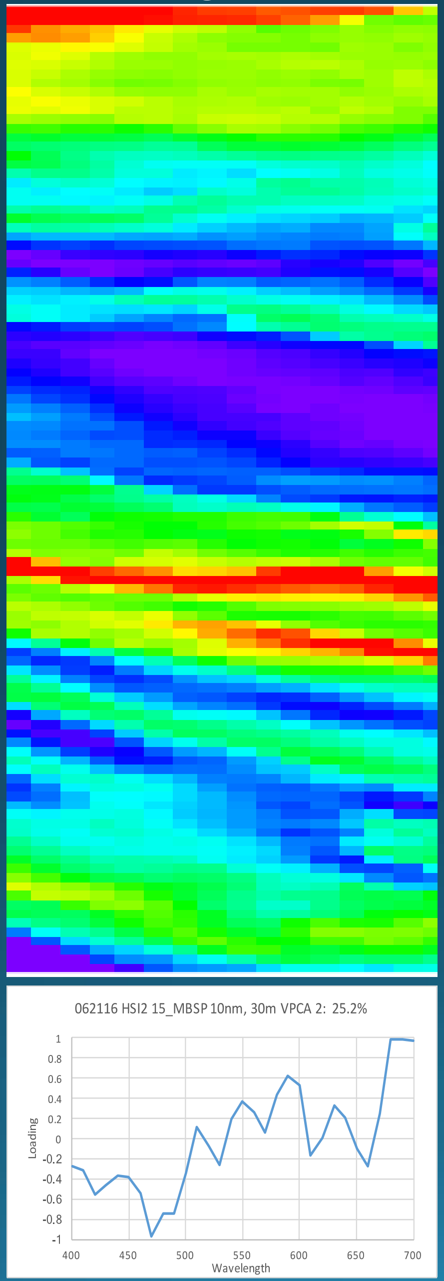

VPCA 2 HSI2 10nm, 3 m, Smooth 9x9

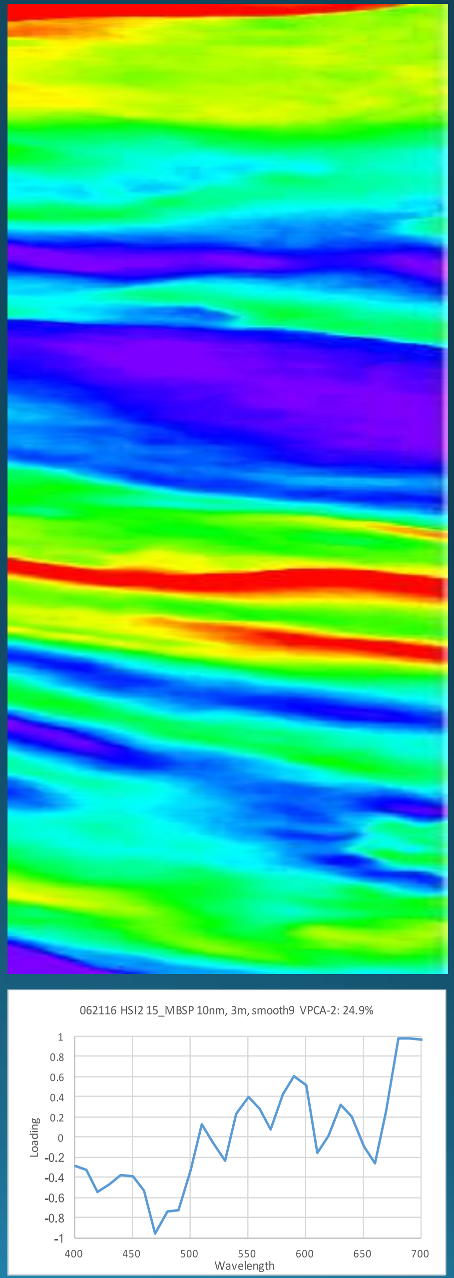

Composition:
Haematite,
Green algae,
-α carotene
and
phycocyanin
(R=0.90)

N

Ortiz et al., (HyspIRI 2017; jortiz@kent.edu)

VPCA 3 Simulated L8 bands, 30m

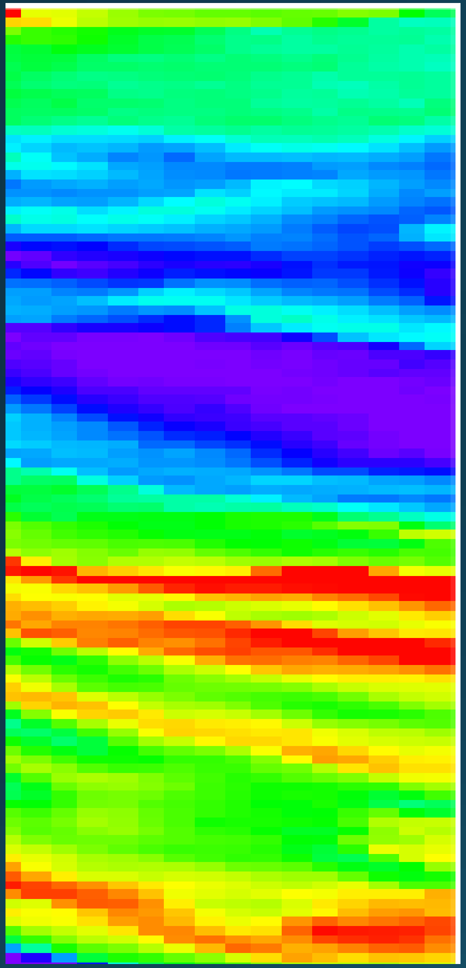

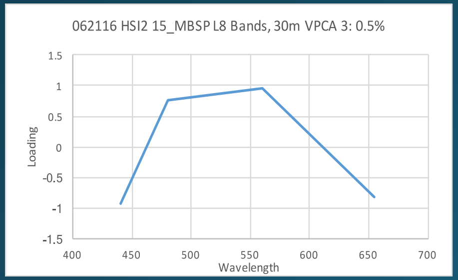

VPCA 3 Simulated L8 bands, 3m, smooth 9x9

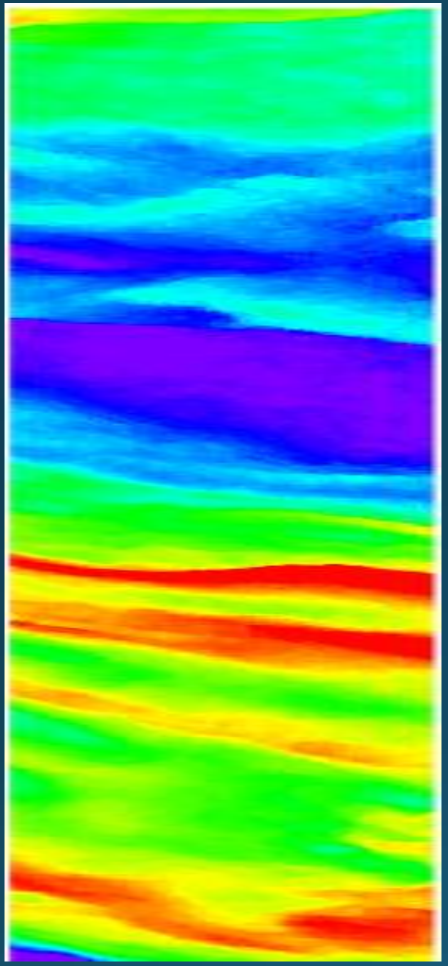

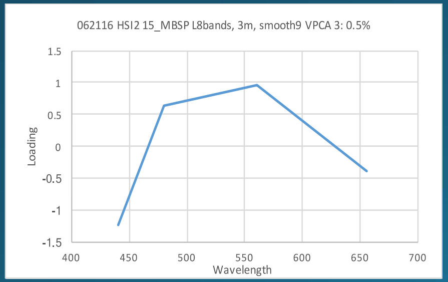

062116 15_MBSP 10nm, 30m, VPCA 3

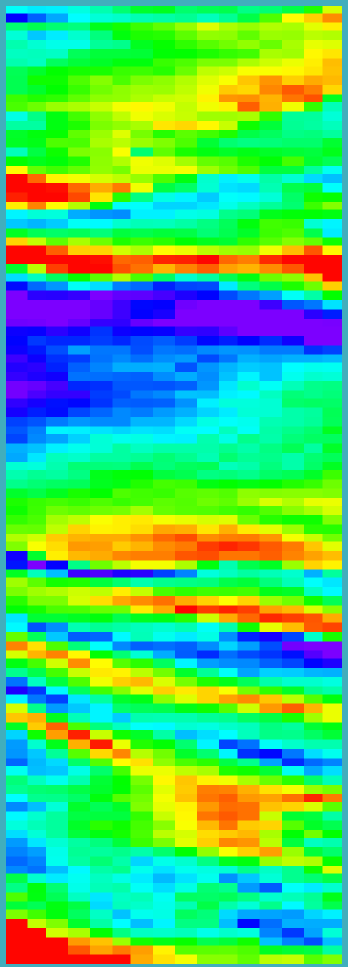

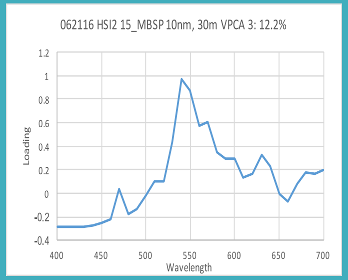

062116 15_MBSP 10nm, 30m, VPCA 4

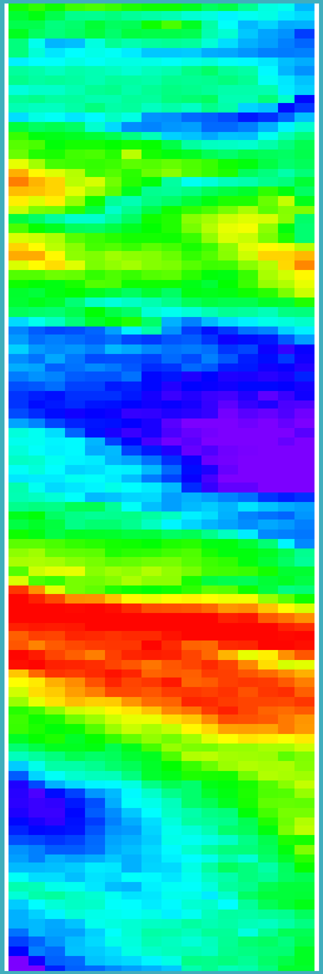

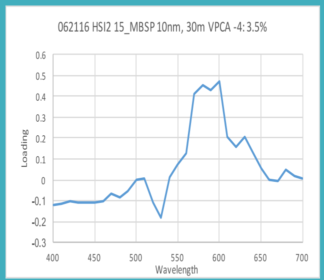

062116 15_MBSP 10nm, 3m, SM9 VPCA-3

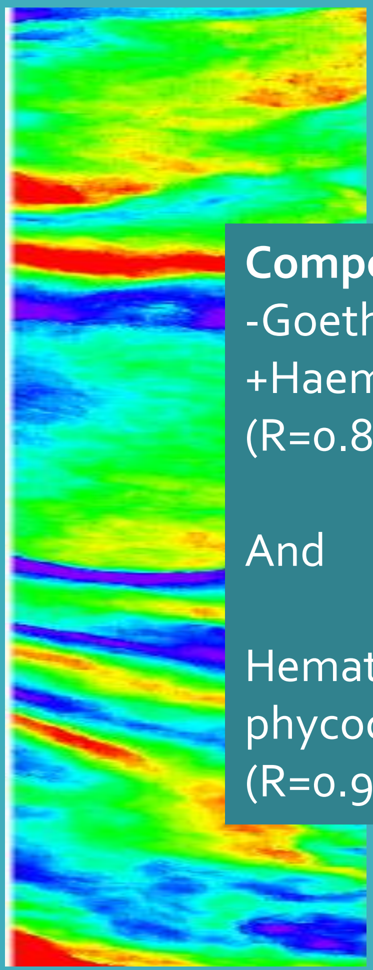

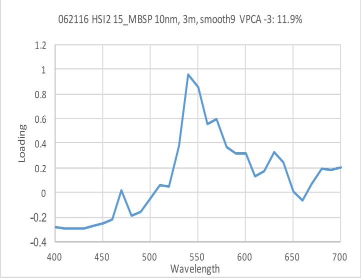

062116 15_MBSP 10nm, 3m, SM9, VPCA 4

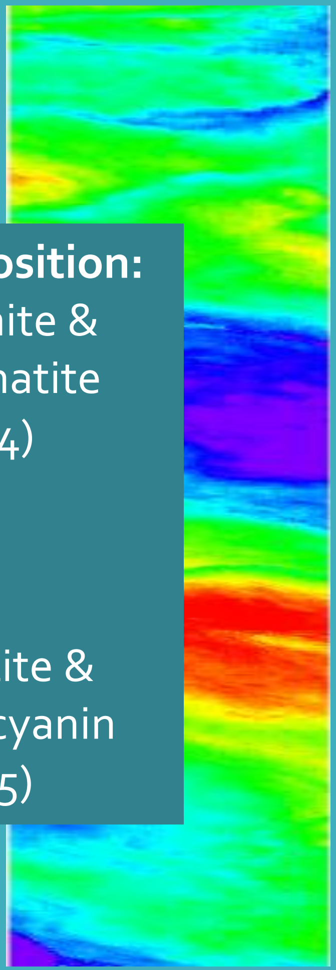

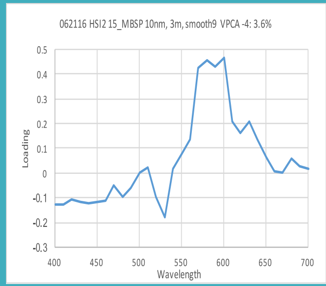

Composition:
-Goethite &
+Haematite
(R=0.84)

And

Hematite &
phycocyanin
(R=0.95)

Actual L8 Image Decomposition

061916 L8 (surface reflectance product), swath15 subset: VPCA decomposition

RGB

061916 L8 swath 15 subset VPCA 1FLIP

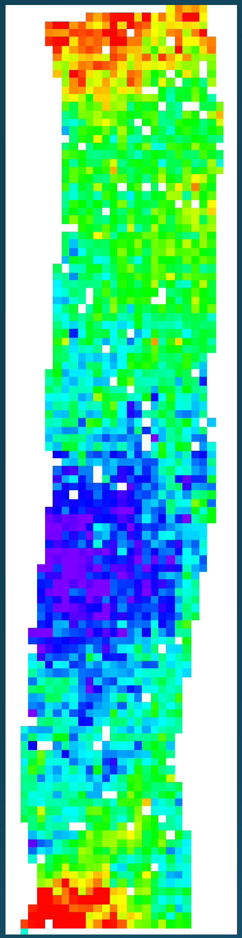

Composition:
Diatoms
(R=0.996)

N

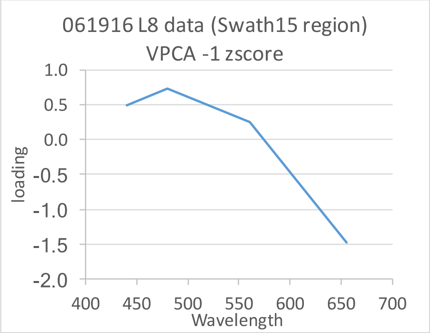

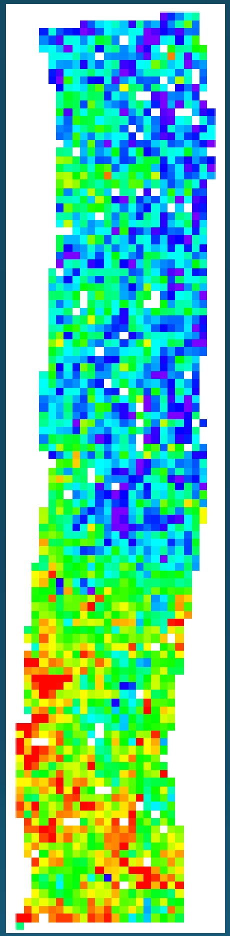

Composition:
Phycocyanin
(R=0.993)

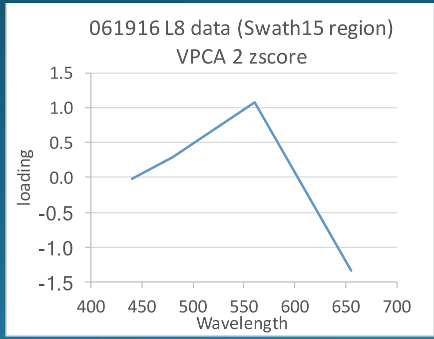

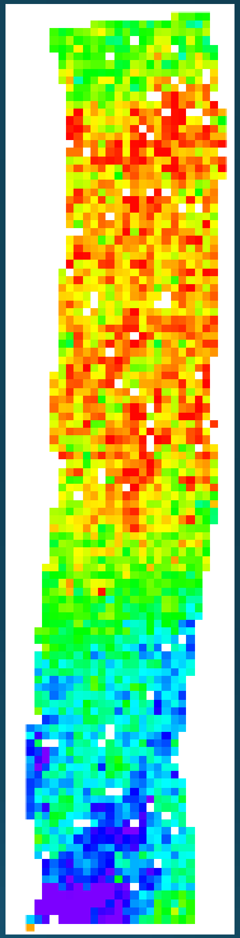

Composition:
Chl a &
carotenoids
(R=0.996)

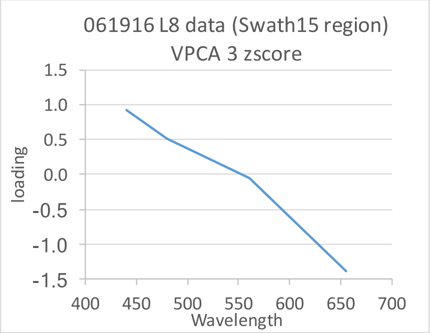

Ortiz et al., (HyspIRI 2017; jortiz@kent.edu)

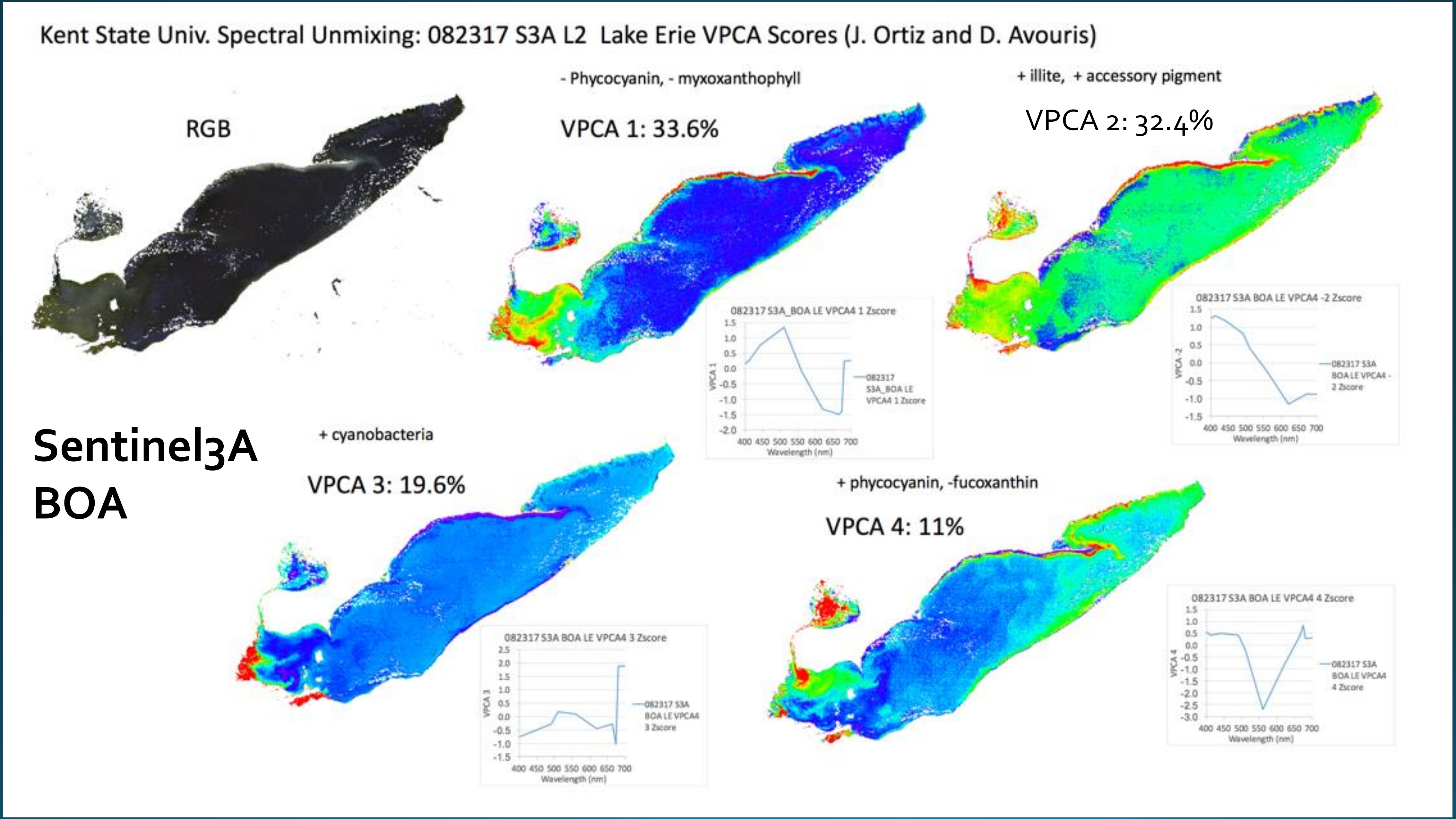

Ortiz et al., (HyspIRI 2017; jortiz@kent.edu)

Sentinel3A Comparison of VPCA to NOAA CI

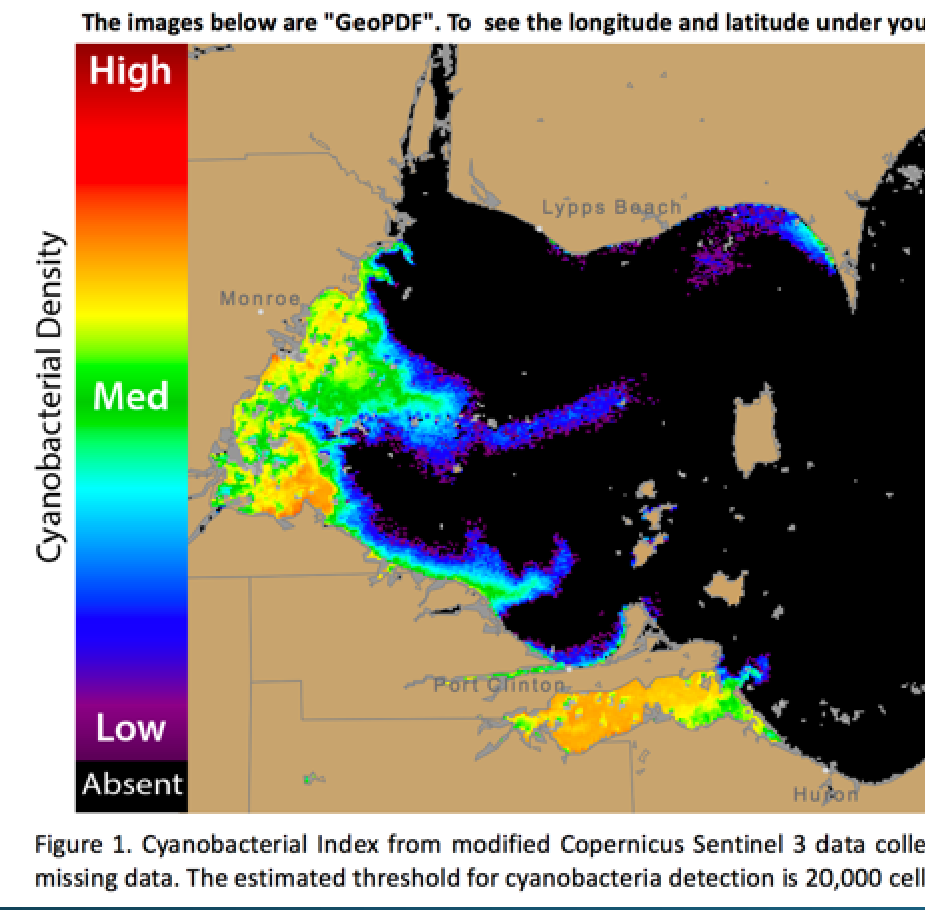

Figure 1. Cyanobacterial Index from modified Copernicus Sentinel 3 data colle
missing data. The estimated threshold for cyanobacteria detection is 20,000 cell

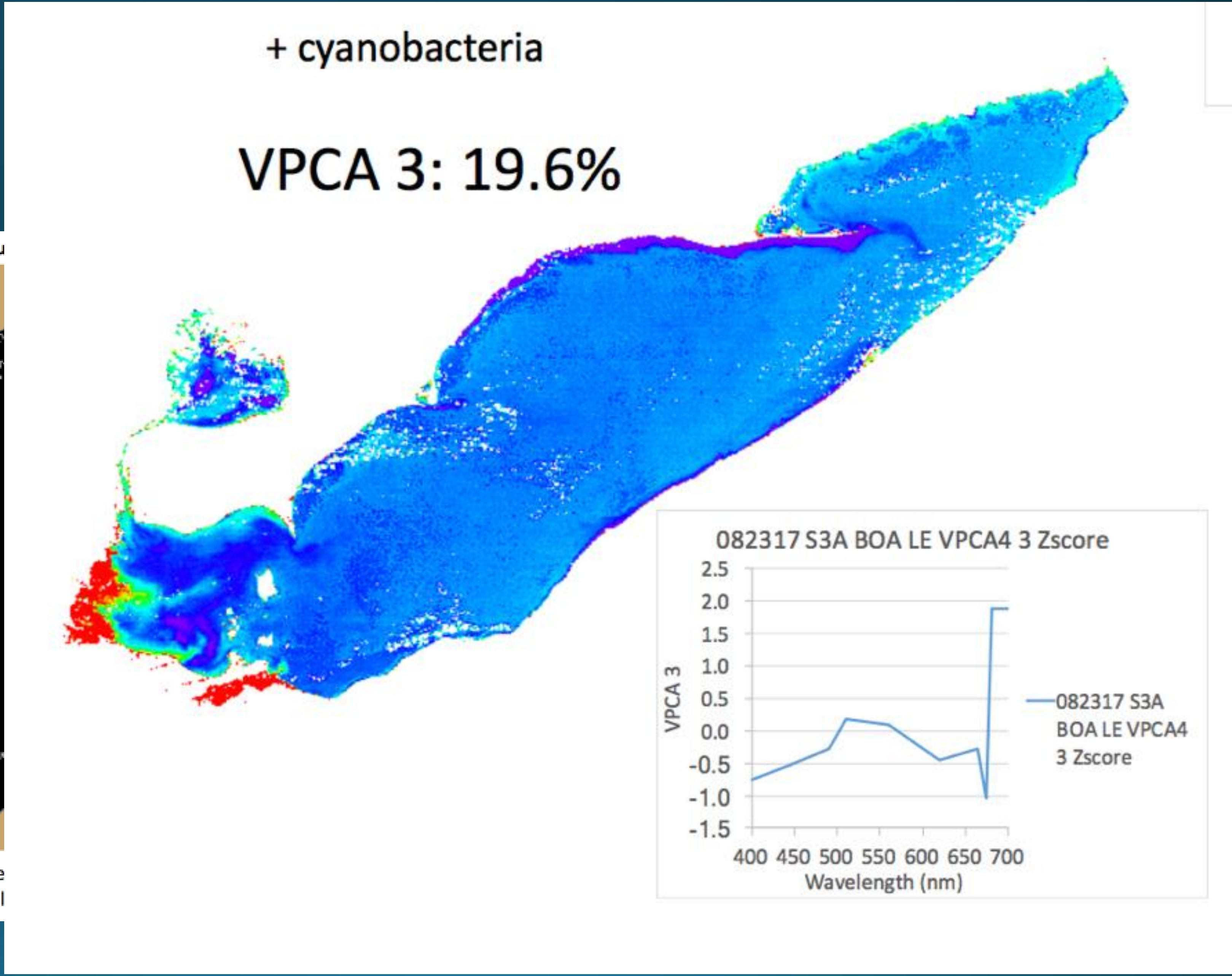

Ortiz et al., (HyspIRI 2017; jortiz@kent.edu)

Conclusions

1. VPCA ties optical assemblages to minerals, phytoplankton and cyanophyte phyla
2. KSU VPCA decomposition method can be applied successfully to Landsat, MODIS, HICO, NASA Glenn HSI2
3. VPCA is well suited for application to Sentinel-3, HyspIRI, PACE: Makes use of ***all*** information present in hyperspectral data
4. The NASA HSI2 (31 visible bands @ 10nm resolution) collects about twice as many components from a simulated L8 scene (with 4 bands in the visible)
5. Spectral decomposition of an actual L8 image collected within two days of the NASA HSI2 swath is consistent with the simulated results
6. Increasing spectral resolution doubles the information that can be partitioned in a scene in terms of the number of extractable components
7. Increasing spatial resolution provides more detailed images, but does not help to extract additional spectral components using this method

Recent Publications

See Water quality webpage at: http://www.personal.kent.edu/~jortiz/home/wqr.html

Ortiz et al., Intercomparison of Approaches to the Empirical Line Method for Vicarious Hyperspectral Reflectance, Front. Mar. Sci., 14 September 2017 | https://doi.org/10.3389/fmars.2017.00296

KA Ali, **J.D.Ortiz**, N Bonini, M Shuman, C Sydow, Application of Aqua MODIS sensor data for estimating chlorophyll a in the turbid Case 2 waters of Lake Erie using bio-optical models, GIScience & Remote Sensing, 1-23, 2016

Ali, K.A., and **J.D. Ortiz**, Multivariate approach for chlorophyll-a and suspended matter retrievals in Case II waters using hyperspectral data, Hydrological Sciences Journal, 2016. DOI 10.1080/02626667.2014.964242.

GS Bullerjahn, et al., Global solutions to regional problems: Collecting global expertise to address the problem of harmful cyanobacterial blooms. A Lake Erie case study, Harmful Algae 54, 223-238, 2016

Ortiz, J.D., Witter, D.L., Ali, K.A., Fela, N., Duff, M., and Mills, L., Evaluating multiple color producing agents in Case II waters from Lake Erie, International Journal of Remote Sensing, 34 (24), 8854-8880, 2013.

Ali, K.A., Witter, D.L., and **J.D. Ortiz**, Application of empirical and semi-analytical algorithms to MERIS data for estimating chlorophyll a in Case waters of Lake Erie, Environmental Earth Sciences; DOI 10.1007/s12665-013-2814-0, published Oct 1, 2013.

Ali, K.A., Witter, D.L., and **J.D. Ortiz**, 2012, Multivariate approach to estimate color producing agents in Case 2 waters using first-derivative spectrophotometer data, Geocarto International, Early online release: 10/30/2012 DOI:10.1080/10106049.2012.743601.

Witter, D., **Ortiz, J.D.,** Palm, S. Heath, R., Budd, J., Assessing the Application of SeaWiFS Ocean Color Algorithms to Lake Erie, Journal of Great Lakes Research, 35, 361-370, 2009.